Enhanced Index Modulation-Based Frequency Hopping: Resist Power-Correlated Reactive Jammer

Yuxin Shi, Kang An, Xinjin Lu, and Yusheng Li

***Abstract*—Reactive jammer has emerged as a relatively intelligent jamming with low energy cost and high jamming efficiency. Moreover, the jammer can obtain the power-correlated reactive jamming via the cooperation with a malicious user, which imposes a severe threat on the reliability of legitimate users. To solve this issue, this letter proposes an enhanced index modulation based frequency hopping spread spectrum (EIM-FHSS) scheme. Specifically, the strategy of power control in EIM-FHSS is provided where the main step of the strategy is formulated as a general optimization problem. Then we calculate a closed form solution for high signal to noise ratio (SNR), and propose a fast search algorithm for general case to obtain the approximate optimal power with low complexity. Simulation results show that EIM-FHSS can obtain enhanced anti-jamming performance as well as low-complexity compared with the benchmarks.**

***Index Terms*—Index modulation, reactive jammer, frequency hopping (FH).**

I. Introduction

THE JAMMER in wireless network aims for preventing legitimate users from accessing wireless network resources and damaging the availability for the legitimate users [1]. Recently, reactive jammer has been regarded as a smart and efficient approach, which only targets the reception of a packet [2]. Compared to proactive jammer, it is hard to detect reactive jammer due to the unknown packet delivery ratio (PDR) in practical scenarios [3]. Using the low-cost software-defined radio (SDR) [4], the reactive jamming enables to configure for several applications.

Frequency hopping spread spectrum (FHSS) has been extensively investigated and regarded as the effective method in anti-jamming communications. FHSS uses the secret FH patterns to determine the available frequencies, which escapes from the jamming signals. However, under the severe threats of the potential fast reactive jamming, the *escape* strategy at frequency becomes hard.

Spatial modulation (SM) is an innovative and promising digital modulation technology, which is also applied in other signal domains such as time/frequency/code domain [5]. In the frequency domain, this concept is termed as index modulation, toward low-complexity, spectrum and energy-efficient next-generation wireless networks [6]. Moreover, this concept has been combined with several anti-jamming schemes such as [7], [8]. In [9], index-modulation based joint mode-frequency-hopping was proposed which activated several orbital angular momentum modes and carrier frequencies to hop simultaneously. Against the above schemes, index modulation based frequency hopping spread spectrum (IM-FHSS) was proposed in [10], which focused on resisting the optimal reactive jamming. However, when the jamming power level is available to be set as legitimate transmit power at the receiver, termed as the *power-correlated* reactive jamming, the performance will be severely damaged.

Focusing on the resistance of the more powerful reactive jamming, an enhanced index modulation based frequency hopping spread spectrum (EIM-FHSS) scheme is proposed in this letter. The main contributions are summarized as follows:

- We consider a novel and challenging jamming scenario, where the jammer is available to employ the power-correlated reactive symbol-level jamming via cooperation with a malicious user. Under this scenario, the traditional IM-FHSS suffers from high bit error rate (BER), which threatens communication reliability.
- The anti-jamming strategy of EIM-FHSS is proposed to resist power-correlated reactive jamming, which is formulated as a general optimization problem. Based on the problem simplification and derivation, a closed form solution for high signal to noise ratio (SNR) regions is obtained.
- For general cases, we further propose a fast search algorithm to obtain the approximate optimal power, which significantly decreases the computational complexity with slight performance loss compared with the traditional ternary search algorithm.

II. Traditional IM-FHSS and Jamming Scenario

A. Basic Structure of IM-FHSS

Since IM-FHSS can resist the reactive jamming under the anti-jamming mode (AJ Mode), we focus on the enhancement of IM-FHSS, AJ Mode in this letter. Assume that m bits information are required to send at each hopping duration. Therefore, the number of available frequencies N is represented by $N = 2^m$. The available frequencies are decided by orthogonal FH patterns which are obtained from the pseudo-random sequence. Then the transmitter selects one frequency from the N frequencies as the active frequency determined by m bits whilst the other $N-1$ frequencies are set as zero, termed as idle frequencies. For example, when $m = 2$ bits, '00'

Manuscript received December 30, 2021; revised January 9, 2022; accepted January 9, 2022. Date of publication January 12, 2022; date of current version April 11, 2022. This work was supported in part by the National Natural Science Foundation of China under Grant U19B214 and Grant 61901502; in part by the Foundation strengthening Plan Area Fund under Grant 2019-JCJQ-JJ-212 and Grant 2019-JCJQ-JJ226; in part by the National Postdoctoral Program for Innovative Talents under Grant BX20200101; and in part by the Research Project of NUDT under Grant ZK18-02-11 and Grant 18-QNCXJ-029. The associate editor coordinating the review of this article and approving it for publication was G. Chen. *(Corresponding author: Yusheng Li.)*

Yuxin Shi, Kang An, and Yusheng Li are with the Sixty-Third Research Institute, National University of Defense Technology, Nanjing 210007, China (e-mail: shiyuxin13@nudt.edu.cn; ankang89@nudt.edu.cn; lys63s@163.com).

Xinjin Lu is with the College of Electronic Science and Technology, National University of Defense Technology, Changsha 410073, China (e-mail: luxinjin17@nudt.edu.cn).

Digital Object Identifier 10.1109/LWC.2022.3142253

and '11' represent the symbol is modulated on the frequency decided by the first and the fourth FH pattern, respectively. Note that information bits are conveyed by the index of the active FH pattern, which is consequently termed as IM-FHSS.

At the receiver, the sampled signals obtained from N available frequencies can be represented by

$$y(k) = \begin{cases} y_A = \sqrt{E}x(k) + n_A(k), \text{ active frequency}, \\ y_I^{(i)} = n_I^{(i)}(k), \text{ idle frequencies}, i = 1, 2, \ldots, N-1, \end{cases} \quad (1)$$

where $y(k) = y(t = kT)$ denotes the sampled signal at kth hopping duration. $x(k)$ is the modulated symbol. Since the utilization of QPSK in IM- FHSS shows better anti-jamming performance for reactive jamming than BPSK, we focus on QPSK in this letter, where $x(k) = \frac{1}{\sqrt{2}}(\pm 1 \pm 1j)$. E is the power level of legitimate signal at the receiver. $n_A(k)$ and $n_I^{(i)}(k)$ denote the additional white Gaussian noise (AWGN) at active frequency and ith idle frequency, respectively.

Subsequently, the energy maximum likelihood (EML) detector is used to distinguish the active frequency from idle ones among N received signals by the energy, and thus

$$\hat{y}_A(k) = \arg\max\left\{ |y_1(k)|^2 |y_2(k)|^2 \ldots |y_N(k)|^2 \right\}, \quad (2)$$

where $y_i(k)$ denotes the sampled signal at ith available frequency. Finally, the index of the $\hat{y}_A(k)$ in FH pattern is used to recover the m bits. Since the idle frequencies are hidden in most unused frequency points, the reactive jammer is unavailable to trace and jam the idle frequencies. Meanwhile, the jamming signal is hard to clean the energy in active frequency in general, and therefore EML detector can effectively distinguish active frequency from idle ones. Consequently, IM-FHSS can resist the most of reactive jamming.

However, once a jammer can obtain the power levels of both present jamming signals and legitimate signals, it is possible for a jammer to clean the energy in active frequency, which threats the communication reliability of IM-FHSS. In the next subsection, we introduce this more challenging scenario and how it works.

B. Jamming Scenario

Under the symbol-level reactive jamming [11], the received signal at the active frequency can be represented by

$$y_A(k) = \begin{cases} \sqrt{E}x(k) + n_A(k), \text{ with probability (w.p.) } 1-\alpha, \\ \sqrt{E}x(k) + J(k) + n_A(k), \text{ w.p. } \alpha, \end{cases} \quad (3)$$

where α denotes the jamming rate. $J(k)$ represents the jamming signals, given by

$$J(k) = \beta \exp(j\Delta\theta)\sqrt{E}z(k), \quad (4)$$

where $z(k)$ has the same modulation type as $x(k)$ for optimal jamming such as $z(k) = \frac{1}{\sqrt{2}}(\pm 1 \pm 1j)$. β and $\Delta\theta$ are the power difference ratio and the phase offset between the jamming signal and legitimate signal, respectively. Here, it can be observed that when the power difference ratio $\beta \approx 1$, i.e., power-correlated jamming, $\sqrt{E}x(k) + J(k)$ will be close to zero at high probability (about 0.25), which causes that the received signal from active frequency is similar to that of idle frequency at the receiver. As a result, the power-correlated reactive jamming can cause the high error rate of IM-FHSS and achieve its jamming goal.

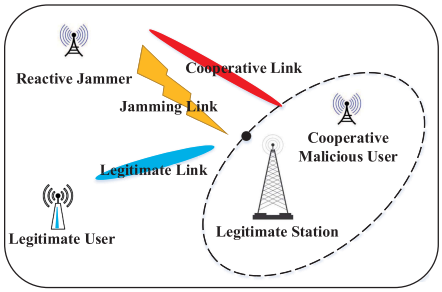

Fig. 1. Jamming scenario under a reactive jammer with cooperation.

Jamming scenario under the cooperative reactive jammer is given in Fig. 1. Specifically, the extra malicious user here is close to the legitimate station, which is available to estimate the power levels of reactive jammer and legitimate user and obtain the power difference ratio. Due to the consistency of the location, it can be assumed that the estimated power difference ratio $\tilde{\beta}$ is the same as the actual β. Then the malicious user secretly transmits $\tilde{\beta}$ to the reactive jammer via the cooperative link. After receiving this information, the reactive jammer adjusts its jamming power, which forms the power-correlated reactive jamming.

III. Strategy of EIM-FHSS and Problem Formulation

A. Strategy of EIM-FHSS

Under the power-correlated reactive jamming, the intuition of solving this issue is to employ the power control algorithm. Specifically, EIM-FHSS can control its transmit power to avoid the power-correlated jamming. Under the intolerable high BER by the threat of reactive jammer, the main strategy of EIM-FHSS can be summarized as the following two steps.

Step 1: If the present transmit power does not obtain the maximum transmit power allowed, EIM-FHSS uses the maximum transmit power allowed.

Step 2: If the present transmit power obtains the maximum transmit power allowed, EIM-FHSS decreases its transmit power guided by the optimization of minimizing the error rate.

Obviously, the legitimate user in *Step 1* uses the maximum transmit power allowed since it can resist both the reactive jamming and AWGN. Hence, the main issue is to determine the optimal transmit power with the minimum error rate in *Step 2*, which is formulated in the next subsection.

B. Problem Formulation and Simplification

According to (3), the received signal at active frequency follows the distribution that

$$y_A \sim \begin{cases} \mathcal{CN}\left(\sqrt{E}, \sigma^2\right), & \text{w.p. } (1-\alpha), \\ \mathcal{CN}\left(\sqrt{E}+\varsigma_1, \sigma^2\right), & \text{w.p. } \frac{\alpha}{4}, \\ \mathcal{CN}\left(\sqrt{E}+\varsigma_2, \sigma^2\right), & \text{w.p. } \frac{\alpha}{4}, \\ \mathcal{CN}\left(\sqrt{E}+\varsigma_3, \sigma^2\right), & \text{w.p. } \frac{\alpha}{4}, \\ \mathcal{CN}\left(\sqrt{E}+\varsigma_4, \sigma^2\right), & \text{w.p. } \frac{\alpha}{4}, \end{cases} \quad (5)$$

where $\varsigma_i = \beta\sqrt{E_0}\exp(j\Delta\theta + (i-1)\frac{\pi}{2}), i = 1,2,3,4$ is introduced by QPSK jamming signal. E_0 denotes the maximum power level as *Step 1*. Using EML detector, the correct detection equals to $\frac{(y_A)^2}{(y_I^{(i)})^2} > 1$ for $i = 1, 2, \ldots, N-1$. Here, the distribution of y_A^2/y_{I}^2 can be computed as [10]

$$y_A^2/y_{\mathrm{I}}^2 \sim \begin{cases} \mathcal{F}\Big(2,2,\frac{E}{\sigma^2/2}\Big), & \text{w.p. } (1-\alpha), \\ \mathcal{F}\Big(2,2,\frac{\tilde{E}_1}{\sigma^2/2}\Big), & \text{w.p. } \frac{\alpha}{4}, \\ \mathcal{F}\Big(2,2,\frac{\tilde{E}_2}{\sigma^2/2}\Big), & \text{w.p. } \frac{\alpha}{4}, \\ \mathcal{F}\Big(2,2,\frac{\tilde{E}_3}{\sigma^2/2}\Big), & \text{w.p. } \frac{\alpha}{4}, \\ \mathcal{F}\Big(2,2,\frac{\tilde{E}_4}{\sigma^2/2}\Big), & \text{w.p. } \frac{\alpha}{4}, \end{cases} \tag{6}$$

where $\mathcal{F}(n_1, n_2, \delta)$ denotes a non-central F-distribution and δ denotes the non-central parameter. n_1 and n_2 present the degree of freedom in numerator and denominator of the random variable, respectively. $\tilde{E}_i$ denotes the power of the received signal under the QPSK jamming signal, given by

$$\begin{aligned} \tilde{E}_i &= \Big(\sqrt{E} + \beta\sqrt{E_0}\cos\Big(\Delta\theta + (i-1)\frac{\pi}{2}\Big)\Big)^2 \\ &+ \Big(\beta\sqrt{E_0}\sin\Big(\Delta\theta + (i-1)\frac{\pi}{2}\Big)\Big)^2 \\ &= E + \beta^2 E_0 + 2\beta\sqrt{EE_0}\cos\Big(\Delta\theta + (i-1)\frac{\pi}{4}\Big). \end{aligned} \tag{7}$$

In the case without the jamming signal at probability of $1-\alpha$, the probability of the erroneous detection is given by

$$P_{e1}(E) = 1 - P_c(E) = 1 - \Big(1 - \psi_2\Big(\frac{E}{\sigma^2/2}\Big)\Big)^{(N-1)}, \tag{8}$$

where $P_c(E)$ denotes the probability of correct detection. $\psi_2(\delta)$ is the simplified form of $\psi(1,2,2,\delta)$, and $\psi(l, n_1, n_2, \delta)$ is the cumulative distribution functions (CDFs) of a non-central F-distribution at the value of *l*.

Similarly, in the case with jamming signal at probability of α, the erroneous detection probability is given by

$$P_{e2} = \frac{1}{4}\sum_{i=1}^{4}\Big(1 - \Big(1 - \psi_2\Big(\frac{\tilde{E}_i}{\sigma^2/2}\Big)\Big)^{(N-1)}\Big). \tag{9}$$

In *Step 2* of EIM-FHSS strategy, the high value of P_I is due to the high P_{e2} derived from the power-correlated jamming. Notice that the main effect on P_{e2} is determined by the worst case, i.e., $\cos(\Delta\theta + (i-1)\frac{\pi}{4}) = -1$ and $\beta = 1$.

Then P_{e2} can be approximate to

$$P_{e2} \approx \frac{1}{4}\Big(1 - \Big(1 - \psi_2\Big(\frac{\tilde{E}_w}{\sigma^2/2}\Big)\Big)^{(N-1)}\Big), \tag{10}$$

where $\tilde{E}_w(E)$ is the worst case for legitimate user, presented by $\tilde{E}_w(E) = (\sqrt{E} - \sqrt{E_0})^2$. Finally, the optimization problem can be formulated as

$$\begin{aligned} E^{\dagger} &= \arg\min_{E} P_I \\ &\text{s.t. : } E \in (0, E_0], \end{aligned} \tag{11}$$

where $P_I = (1-\alpha)P_{e1} + \alpha P_{e2}$ denotes the total index error rate. Note that problem (11) is hard to directly obtain the closed form solution since the objective function P_I is complex. Without loss of generality, we set $E_0 = 1$ in the following discussion.

Remark 1: It is worth noting that the power control in EIM-FHSS is sensitive to the complexity since the reactive jammer may adjust its jamming power as soon as possible to keep employing power-correlated jamming. If the processing time of the solving (11) is longer than the cooperative time of the jammer, the legitimate receiver will suffer from the power-correlated jamming in most of time. Hence, the low-complexity solving or search algorithm is required for this scenario.

IV. Solution to Optimization Problem

A. Approximate Solution at High SNR Regions

To obtain the optimal E_{op}, we calculate the derivative

$$\begin{aligned} \frac{\partial P_I}{\partial E} &= (1-\alpha)\frac{\partial P_{e1}}{\partial E} + \alpha\frac{\partial P_{e2}}{\partial E}, \\ &= (1-\alpha)\frac{\partial P_{e1}}{\partial \delta_1}\frac{\partial \delta_1}{\partial E} + \alpha\frac{\partial P_{e2}}{\partial \delta_2}\frac{\partial \delta_2}{\partial E}, \\ &\approx (1-\alpha)(N-1)(1-\psi_2(\delta_1))^{N-2}\frac{\partial \psi_2(\delta_1)}{\partial \delta_1}\frac{\partial \delta_1}{\partial E} \\ &+ \frac{\alpha}{4}(N-1)(1-\psi_2(\delta_2))^{N-2}\frac{\partial \psi_2(\delta_2)}{\partial \delta_2}\frac{\partial \delta_2}{\partial E}, \end{aligned} \tag{12}$$

where $\delta_1 = \frac{E}{N_0/2}$ and $\delta_2 = \frac{(\sqrt{E}-\sqrt{E_0})^2}{N_0/2}$ denote the non-central parameters of $\psi_2(\cdot)$ in P_{e1} and P_{e2}, respectively.

Theorem 1: The $\psi_2(\delta)$ and its derivative $\frac{\partial \psi_2(\delta)}{\partial \delta}$ can be represented by

$$\psi_2(\delta) = \sum_{j=0}^{\infty}\frac{\big(\frac{1}{4}\delta\big)^j}{j!}\frac{1}{2}e^{-\frac{\delta}{2}}, \frac{\partial \psi_2(\delta)}{\partial \delta} = -\sum_{j=0}^{\infty}\frac{1}{8}\frac{\big(\frac{1}{4}\delta\big)^j}{j!}e^{-\frac{\delta}{2}}. \tag{13}$$

Proof: The representations of $\psi(l, \nu_1, \nu_2, \delta)$ can be represented by [12]

$$\psi(l,\nu_1,\nu_2,\delta) = \sum_{j=0}^{\infty}\frac{\big(\frac{1}{2}\delta\big)^j}{j!}e^{-\frac{\delta}{2}}I\Big(\frac{n_1 l}{n_2 + n_1 l}\Big|\frac{n_1}{2} + j, \frac{n_2}{2}\Big), \tag{14}$$

where $I(x|z., w)$ denotes the incomplete beta function, i.e.,

$$I(x|z\,, w) = \frac{1}{B(z,w)}\int_0^x t^{z-1}(1-t)^{w-1}dt, \tag{15}$$

where *B*(*z*, *w*) denotes the beta function, and $B(z,w) = int_0^1\, t^{z-1}(1-t)^{w-1}dt$. Substituting $n_1 = 2$, $n_2 = 2$ and $l = 1$ into (15), we obtain that $B(z,w) = \frac{1}{j+1}$ and $I(x|z,w) = (\frac{1}{2})^{j+1}$. Then $\psi_2(\delta)$ is given by

$$\psi_2(\delta) = \sum_{j=0}^{\infty}\Upsilon_j(\delta), \tag{16}$$

where $\Upsilon_j(\delta) = \frac{(\frac{1}{4}\delta)^j}{j!}\frac{1}{2}e^{-\frac{\delta}{2}}$. Subsequently, the derivative of $\psi_2(\delta)$ can be calculated by

$$\begin{aligned} \frac{\partial \psi_2(\delta)}{\partial \delta} &= \frac{\partial \Upsilon_0(\delta)}{\partial \delta} + \sum_{j=1}^{\infty}\frac{\partial \Upsilon_j(\delta)}{\partial \delta} \\ &= -\frac{1}{4}e^{-\frac{\delta}{2}} + \sum_{j=1}^{\infty}\Big(\frac{1}{8}\frac{\big(\frac{1}{4}\delta\big)^{j-1}}{(j-1)!}e^{-\frac{\delta}{2}} - \frac{1}{4}\frac{\big(\frac{1}{4}\delta\big)^j}{j!}e^{-\frac{\delta}{2}}\Big) \end{aligned}$$

$$= -\sum_{j=0}^{\infty} \frac{1}{8} \frac{\left(\frac{1}{4}\delta\right)^j}{j!} e^{\frac{-\delta}{2}}. \quad (17)$$

■

Next, the first term in (17) is used as an approximate form of $\frac{\partial \psi_2(\delta)}{\partial \delta}$, and $\frac{\partial P_I}{\partial E} = 0$ can be further represented by

$$(1-\alpha)(1-\psi_2(\delta_1))^{N-2} \exp\left(-\frac{E}{N_0}\right) = \frac{\alpha}{4}\left(\frac{1}{\sqrt{E}} - 1\right)(1-\psi_2(\delta_2))^{N-2} \exp\left(-\frac{\left(\sqrt{E}-1\right)^2}{N_0}\right). \quad (18)$$

Then we take the logarithm of (18), and thus

$$\ln\left(\frac{4(1-\alpha)}{\alpha}\right) + (N-2)\ln\left(\frac{1-\psi_2(\delta_1)}{1-\psi_2(\delta_2)}\right) - \ln\left(\frac{1}{\sqrt{E}} - 1\right) + \frac{1-2\sqrt{E}}{N_0} = 0. \quad (19)$$

We observe that it is still hard to obtain the closed form solution via (19). Fortunately, (19) can be further transformed into a simple form since $\psi_2(\delta_1)$, $\psi_2(\delta_2)$ and N_0 are very close to 0 at high SNR regions. Then (19) can be simplified to

$$1 - 2\sqrt{E} = 0. \quad (20)$$

Finally, we calculate that $E_{op} \approx 0.25$ at high SNR regions.

B. Solution Based on Fast Ternary Search

Since high SNR conditions may not be always met in real scenarios, we propose a general and fast method to obtain the solution $E^{\dagger}$. When the power control is not employed where $E = E_0$ as IM-FHSS, we obtain that $\tilde{E}_w(1) = 0$ and $\psi_2(0) = 0.5$ in (10), leading to high P_I. On the contrary, when E is close to 0, $P_c(E)$ in (8) is close to 0.5^{N-1}, which leads to high P_I. According to the analysis above, the objective function may be a *convex function*. Hence, the ternary search can be utilized for the power control, which is efficient for searching the minimum of a *convex function* [13].

To further obtain the low complexity as Remark 1, the fast search algorithm is proposed in Algorithm 1. E_l and E_r are the left endpoint and right endpoint of E, respectively. The midpoint and three quarters point of the present zone are E_{mid_1} and E_{mid_2}, respectively. After comparing the values of objective functions calculated by E_{mid_1} and E_{mid_2}, E_{mid_1} is set as the new boundary of the present zone. While the present zone is smaller than a constant ϵ, the optimal power E_{op} calculated by the average of E_{mid_1} and E_{mid_2} is output.

Different from the traditional ternary search using the trisection points, the proposed search algorithm uses the midpoint and three quarters point as the comparative points. In addition, the midpoint is set as the only new boundary, which increases the iteration speed and decreases computational complexity. The computational complexity is further discussed in the next subsection.

C. Computational Complexity Analysis

Recall that the computational complexity is mainly derived from the calculation of $P_I(E_{mid_1})$ and $P_I(E_{mid_2})$. Also, first K terms in (16) can be used to approximate $\psi_2(\delta)$ in P_I. Here,

Algorithm 1 The Proposed Search Algorithm for EIM-FHSS

Input: E_l and E_r are initially set as 0 and 1, respectively. ϵ denotes the largest zone allowed for the end of while-loop.

```
while E_r − E_l > ε do
    E_mid1 = (1/2)(E_l + E_r);
    E_mid2 = (1/2)(E_mid1 + E_r);
    if P_I(E_mid1) < P_I(E_mid2) then
        E_r = E_mid1;
    else
        E_l = E_mid1;
    end if
end while
E_op = (E_mid1 + E_mid2)/2;
```

Output: E_{op};

the computational complexity of calculating $\psi_2(\delta)$ is mainly at $\sum_{j=0}^{K} \frac{(\frac{1}{4}\delta)^j}{j!}$, which can be represented by $\sim \mathcal{O}(K^2)$ in terms of multiplications. In order to calculate P_I, the corresponding computational complexity c_{P_I} is $\sim \mathcal{O}(K^2 + N)$. For convenience, we assume the calculation of one P_I is a complexity unit and investigate the decrease of computational complexity of Algorithm 1 as follows.

Theorem 2: For a given ϵ, the complexity of the proposed algorithm is

$$C = 2\left\lceil \log_2\left(\frac{E_0}{\epsilon}\right)\right\rceil. \quad (21)$$

Proof: The initial zone of $E \in [0, E_0]$ is E_0. At each iteration, the zone is reduced by half, and thus the condition of jumping out the while-loop can be represented by $\frac{E_0}{2^M} < \epsilon$, where M denotes the number of iterations which meets the condition of jumping out the while-loop. Then we obtain that the smallest number of iterations

$$\bar{M} = \left\lceil \log_2\left(\frac{E_0}{\epsilon}\right)\right\rceil. \quad (22)$$

Since the proposed algorithm calculates the objective function P_I twice at each iteration, it is obvious that $C = 2\bar{M}$. ■

Using Theorem 2, the complexity of the traditional ternary search can be also obtained, given by

$$C_t = 2\left\lceil \log_{\frac{3}{2}}\left(\frac{E_0}{\epsilon}\right)\right\rceil. \quad (23)$$

Then the ratio of the complexity between these two algorithms is represented by

$$\gamma = \frac{C}{C_t} = \frac{\left\lceil \log_2\left(\frac{E_0}{\epsilon}\right)\right\rceil}{\left\lceil \log_{\frac{3}{2}}\left(\frac{E_0}{\epsilon}\right)\right\rceil} \approx \frac{\log_2\left(\frac{E_0}{\epsilon}\right)}{\log_{\frac{3}{2}}\left(\frac{E_0}{\epsilon}\right)} = \log_2\left(\frac{3}{2}\right). \quad (24)$$

Therefore, the proposed algorithm can decrease computational complexity to 58.5% compared with traditional ternary search.

V. Simulation Results

In this section, the signal to noise ratio (SNR) here is given by $\text{SNR (dB)} = 10\log_{10}(\frac{1}{N_0})$. The largest zone allowed ϵ is set as 0.05. For convenience, we set $N = 2$ in the simulations.

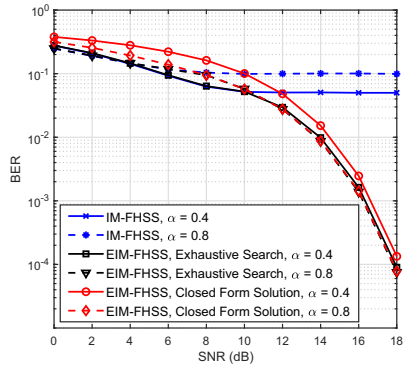

Fig. 2. BER comparisons among IM-FHSS, EIM-FHSS with exhaustive search and closed form solution at $\alpha = 0.4$ and 0.8.

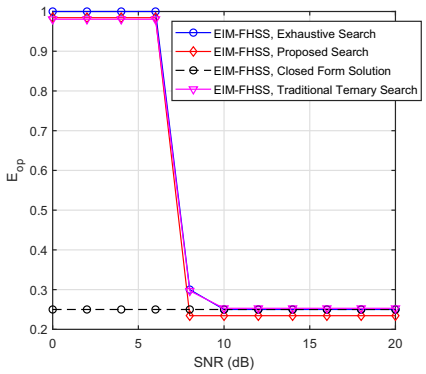

Fig. 3. Estimated optimal power of the exhaustive search, the proposed search, the closed form solution and the ternary search in EIM-FHSS at $\alpha = 0.8$.

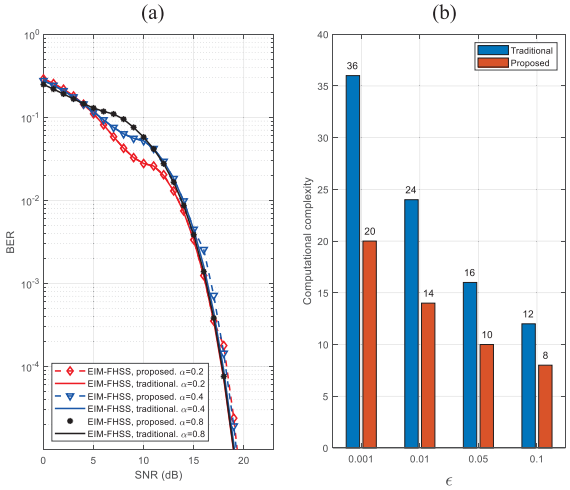

Fig. 4. Comparisons of EIM-FHSS, AJ Mode, QPSK using the traditional ternary search and the proposed search algorithm. (a) BER comparison. (b) Computational complexity comparison.

In Fig. 2, it can be observed that IM-FHSS suffers from the error floor, since the power of IM-FHSS remains power under power-correlated jamming. Here, EIM-FHSS with exhaustive search provides the minimum BER as a benchmark. We observe that EIM-FHSS with closed form solution is approximate to the exhaustive search, which validates the correctness of the derivatives.

In Fig. 3, the estimated optimal power of exhaustive search, the proposed search, the closed form solution and the ternary search in EIM-FHSS are provided under $\alpha = 0.8$. We observe that the ternary search is very closed to the exhaustive search. Also, the power control of the proposed search is approximate to the exhaustive search. Moreover, the closed form solution fits well with the exhaustive search when SNR>10dB.

In Fig. 4 (a), it can be seen that the proposed search algorithm only suffers slight performance loss at high SNR region. Fig. 4 (b) shows the comparisons of computational complexity between the proposed search algorithm and the traditional ternary search under different values of ϵ. Then we obtain the simulated ratio $\hat{\gamma} = 55.6\%$, 58.33%, 62.5% and 66.7%, which confirms the correctness of Eq. (24). Combining Fig. 4 (a) and Fig. 4 (b), we conclude that the proposed search algorithm can significantly decrease the computational complexity with slight performance loss.

VI. Conclusion

In this letter, we considered a power-correlated reactive symbol-level jamming scenario, which threatens IM-FHSS scheme. We formulated this scenario to an optimization problem and proposed a closed form solution for high SNR regions and a fast search algorithm for general case. Simulation results showed that EIM-FHSS outperformed IM-FHSS under power-correlated reactive jamming and significantly decreased computational complexity compared to the benchmark.

References

[1] Y. Zou, J. Zhu, X. Wang, and L. Hanzo, "A survey on wireless security: Technical challenges, recent advances, and future trends," *Proc. IEEE*, vol. 104, no. 9, pp. 1727–1765, Sep. 2016.

[2] K. Pelechrinis, M. Iliofotou, and S. V. Krishnamurthy, "Denial of service attacks in wireless networks: The case of jammers," *IEEE Commun. Surveys Tuts.*, vol. 13, no. 2, pp. 245–257, 2nd Quart., 2011.

[3] K. Grover, A. Lim, and Q. Yang, "Jamming and anti-jamming techniques in wireless networks: A survey," *Int. J. Ad Hoc Ubiquitous Comput.*, vol. 17, no. 4, pp. 197–215, 2014.

[4] M. Wilhelm, I. Martinovic, J. B. Schmitt, and V. Lenders, "Short paper: Reactive jamming in wireless networks: how realistic is the threat?," in *Proc. ACM Conf. Wireless Netw. Security*, 2011, pp. 1–6.

[5] M. Wen *et al.*, "A survey on spatial modulation in emerging wireless systems: Research progresses and applications," *IEEE J. Sel. Areas Commun.*, vol. 37, no. 9, pp. 1949–1972, Sep. 2019.

[6] E. Basar, M. Wen, R. Mesleh, M. Di Renzo, Y. Xiao, and H. Haas, "Index modulation techniques for next-generation wireless networks," *IEEE Access*, vol. 5, pp. 16693–16746, 2017.

[7] E. Basar, U. Aygolu, E. Panayirci, and H. V. Poor, "Orthogonal frequency division multiplexing with index modulation," *IEEE Trans. Signal Process*, vol. 61, no. 22, pp. 5536–5549, Nov. 2013.

[8] G. Kaddoum, Y. Nijsure, and H. Tran, "Generalized code index modulation technique for high-data-rate communication systems," *IEEE Trans. Veh. Technol.*, vol. 65, no. 9, pp. 7000–7009, Sep. 2016.

[9] L. Liang, W. Cheng, and H. Zhang, "Index modulation based joint mode-frequency hopping," *IEEE Commun. Lett.*, vol. 25, no. 6, pp. 1810–1814, Jun. 2021.

[10] Y. Shi, K. An, and Y. Li, "Index modulation based frequency hopping: Anti-jamming design and analysis," *IEEE Trans. Veh. Technol.*, vol. 70, no. 7, pp. 6930–6942, Jul. 2021.

[11] H. S. Jang and B. C. Jung, "Performance analysis of reactive symbol-level jamming techniques," *IEEE Trans. Veh. Technol.*, vol. 67, no. 12, pp. 12432–12437, Dec. 2018.

[12] N. L. Johnson, S. Kotz, and N. Balakrishnan, "Continuous univariate distributions," *J. Amer. Stat. Assoc.*, vol. 1, p. 756, Oct. 1994. [Online]. Available: https://rss.onlinelibrary.wiley.com/doi/abs/10.2307/2983186

[13] M. S. Bajwa, A. P. Agarwal, and S. Manchanda, "Ternary search algorithm: Improvement of binary search," in *Proc. 2nd Int. Conf. Comput. Sustain. Global Develop. (INDIACom)*, 2015, pp. 1723–1725.